

Polyphosphazenes Functionalized with Sulfone or Sulfoxide Groups: Synthesis, Characterization, and Possible Polymer Electrolyte Applications

Harry R. Allcock* and David L. Olmeijer

Department of Chemistry, The Pennsylvania State University, University Park, Pennsylvania 16802

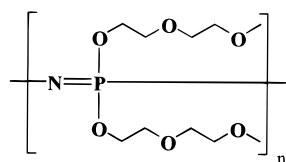
Received May 12, 1998; Revised Manuscript Received August 31, 1998

ABSTRACT: A method for the introduction of sulfone or sulfoxide functional groups into the side groups of polyphosphazenes has been developed. This procedure involves the prior introduction of thioether-containing side groups into phosphazenes followed by oxidation of the sulfur atoms by H_2O_2 or *m*-chloroperbenzoic acid (MCPBA). This method was first explored at the level of model small molecule cyclic species as a prelude to the polymer oxidation reactions. The attractive forces generated by sulfone or sulfoxide functional groups produce alkyloxy-substituted polyphosphazenes with relatively high glass transition temperatures (up to $+19^\circ\text{C}$). The potential of these materials as polymer electrolytes, both in the solid state and in systems with added propylene carbonate, was explored by means of impedance analysis conductivity studies. The competition between the polymer and the solvent for lithium ions was also investigated.

Introduction

Considerable research has been reported on polymer electrolytes for use in secondary lithium and lithium ion batteries. Lithium batteries with nonplasticized polymer electrolytes have advantages over those that contain small-molecule organic solvents. Such solvents are volatile and can lead to pressure buildup, leakage, lack of dimensional stability, and flammability. Nonplasticized polymers also have significant advantages over liquid electrolytes in that they expand the options available for battery design, including processing into thin films and intricate shapes to give batteries that can conform to the dimensions of any device.

Secondary lithium batteries using solid polymer electrolytes (SPEs) have been investigated since 1978,^{1,2} following the report by Wright of the formation of complexes between poly(ethylene oxide) (PEO) and potassium thiocyanate salts.^{3–5} In 1984, Blonsky, Shriver, Austin, and Allcock reported the synthesis and study of poly[bis(2-(2-methoxyethoxy)ethoxy)phosphazene] (MEEP, **1**) as a low glass-transition tempera-



1 (MEEP)

ture, amorphous polymer which overcomes many of the shortcomings associated with PEO.^{6,7} When complexed to LiSO_3CF_3 , MEEP has an ambient temperature ionic conductivity in the range of 10^{-5} S/cm, which is 2–3 orders of magnitude higher than that for PEO. In recent years, more than 30 new polyphosphazenes for ionic conduction have been synthesized in our program, including species with an increased number of oxygen atoms per side unit, others that utilize branched rather than linear oligo(oxyethylene) side groups, examples that use non-ion-coordinating cosubstituents, and poly-

mers which incorporate crown ethers.^{8–13} MEEP–PEO blends have also been investigated.^{14,15} Some of these systems improve the ionic conductivity and have higher dimensional stability than MEEP. Furthermore, polyphosphazene-based solid electrolytes have been shown to be stable to lithium metal anodes.¹⁶

Practical battery applications require ionic conductivities in the range of 10^{-3} S/cm. Even the best solid polymer electrolyte–salt complexes have ionic conductivities in the region of 10^{-5} S/cm. For this reason, many researchers have studied gel–electrolyte systems, in which polar organic solvents such as propylene carbonate, sulfolane, dimethyl sulfoxide, or dimethyl formamide are used to swell a host polymer matrix, which then serves mainly to provide structural integrity.^{17,18} The polymer most often studied for this purpose has been polyacrylonitrile (PAN), but similar studies have been performed on PEO^{19,20} and SiO_2 matrixes.²¹ In our program, MEEP– LiSO_3CF_3 systems have been studied with propylene carbonate, *N*-methylpyrrolidone, or nonvolatile small-molecule cyclotriphosphazene-based additives, and conductivities as high as 10^{-3} S/cm have been measured.²²

Organic molecules that contain sulfone or sulfoxide functional groups have some of the highest dipole moments and dielectric constants known. Table 1 compares the dipole moments of analogous compounds with different nonionic functional groups.²³ Polymers, such as poly(vinyl sulfone) (PVS), have been studied for use both as solid polymer electrolytes and in gel-type systems.^{24–27} PVS is a highly cross-linked glassy material with low ionic conductivity when complexed with $\text{LiN}(\text{SO}_2\text{CF}_3)_2$. However, when it is plasticized with propylene carbonate or sulfolane, ionic conductivities up to 3.7×10^{-4} S/cm at 25°C are obtained.^{25,26}

Polyphosphazenes have been functionalized with a wide variety of ionic, nonionic, reactive, and unreactive organic functional groups, including carboxylic acids,^{28,29} sulfonic acids,^{30–32} primary, secondary, and tertiary amines,^{33,34} alcohols,^{35,36} ethers,³⁷ and thioethers.^{38,39} There have been few reports of the attempted incorpo-

Table 1. Dipole Moments of Some Related Organic Molecules²³

molecule	functionality	dipole moment (D)
CH ₃ S(O) ₂ CH ₃	sulfone	4.49
CH ₃ S(O)CH ₃	sulfoxide	3.96
CH ₃ C(O)CH ₃	ketone	2.88
CH ₃ SCH ₃	thioether	1.50
CH ₃ OCH ₃	ether	1.30

ration of sulfone or sulfoxide functional groups into polyphosphazenes. Allcock and Austin reported the synthesis of phosphazene cyclic trimers containing sulfadiazine groups following a Schiff base coupling reaction.⁴⁰ In a separate instance, Hergenrother and Halasa described the formation of a direct phosphorus-carbon bond during the reaction of sulfones with poly-(dichlorophosphazene) in the presence of an HCl acceptor. However, the product contained a maximum of only 5% sulfone substitution and decomposed through hydrolysis of P-Cl bonds.⁴¹ There have been no reports of polyphosphazenes functionalized with sulfoxide groups.

An aim of this project was to develop a synthetic methodology to introduce sulfone and sulfoxide groups into polyphosphazenes. Model experiments were first carried out with cyclic phosphazene trimers before the counterpart reactions were attempted at the macromolecular level. The methodology was then applied to the high polymers, which were characterized with respect to their thermal properties and then evaluated for ionic conductivity for possible use as both solid polymer electrolytes and host materials for gel-electrolyte applications.

Results and Discussion

Synthesis by Direct Substitution. Initially, the most logical synthetic approach for the incorporation of sulfone groups into polyphosphazenes seemed to be via the replacement of chlorine in chlorophosphazenes using sodium 2-(methylsulfonyl)ethoxide as a nucleophile. Model reactions involving hexachlorocyclotriphosphazene (N₃P₃Cl₆, **2**) and N₃P₃(OC₆H₅)₅Cl (**3**) showed that neither interaction gave the expected product. Indeed, ³¹P NMR studies revealed a complex series of reactions which probably involved the sulfonyl moiety.

Synthesis by Oxidation of Thioethers. Because of the complexity of the reaction described above, an alternative approach was taken to link sulfone-bearing side groups to phosphazenes. Small-molecule and high polymeric phosphazenes were prepared with alkyloxy side groups that contained terminal thioether units, which were then exposed to oxidizing agents. Again, model reactions were carried out on cyclotriphosphazenes before use at the macromolecular level.

Pentaphenoxy Cyclic Trimers. Replacement of the chlorine atom in **3** was carried out by reaction with sodium 2-(methylthio)ethoxide to produce N₃P₃(OC₆H₅)₅-(OCH₂CH₂SCH₃) (**4**) (Scheme 1). Potassium peroxy-monosulfate (Oxone, 2KHSO₅·K₂SO₄·KHSO₄) was used as the oxidizing agent according to a technique reported previously.⁴² This reaction produced both N₃P₃(OC₆H₅)₅-(OCH₂CH₂S(O)CH₃) (**5**) and N₃P₃(OC₆H₅)₅-(OCH₂CH₂-S(O)₂CH₃) (**6**), indicating the incomplete oxidation of some thioether groups to the sulfoxide. Subsequent oxidation of this mixture yielded **6** as the only product (Scheme 1).

Hexasubstituted Cyclotriphosphazenes. Attempts were then made to perform similar reactions on hexakis-(2-methylthioethoxy)cyclotriphosphazene (**7**) (Scheme 2).

Initial experiments using Oxone as the oxidizing agent were unsuccessful. The acidic conditions associated with this oxidizing agent cleaved the phosphazene trimer ring, presumably because it lacked the bulky protective phenoxy groups of **4**. Thus, the ring nitrogen atoms were susceptible to attack by H⁺. Use of a pH = 7 buffer during the oxidation reaction was also unsuccessful.

Oxidation of **7** was accomplished by carrying out the oxidation reaction with H₂O₂ (Scheme 2). At ambient temperatures, the oxidation proceeded via the intermediate hexakis-(2-methylsulfoxyethoxy)cyclotriphosphazene (**8**), without overoxidation to the sulfone. Compound **8** was not purified from residual excess H₂O₂ and therefore was further oxidized in the solid state to hexakis-(2-methylsulfonylethoxy)cyclotriphosphazene (**9**). Infrared spectroscopy confirmed the presence of this functional group (Figure 1). Synthesis of **9** could also be accomplished directly (without detection of the intermediate **8**) by performing the oxidation reaction with 35% H₂O₂ in refluxing methanol.

High Polymeric Phosphazenes. Because the oxidation of thioethers linked to small-molecule cyclic phosphazene trimers was successful, the final step was to attempt similar reactions at the macromolecular level to give sulfoxide- or sulfone-functionalized phosphazene high polymers.

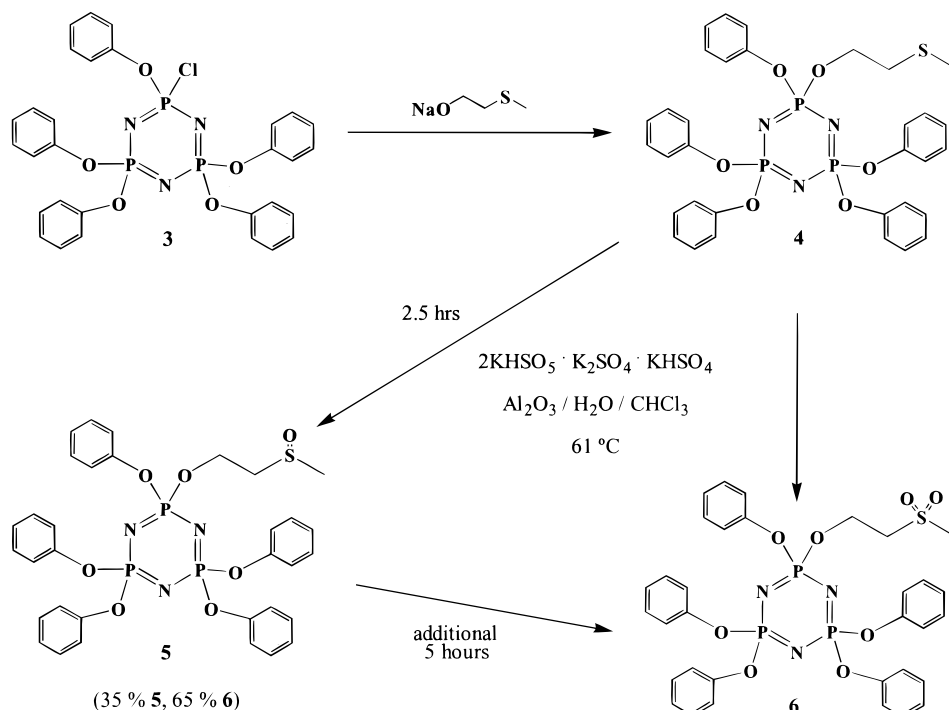
Poly(dichlorophosphazene) (**10**) was treated with sodium 2-(methylthio)ethoxide in THF solution to produce poly[bis(2-methylthioethoxy)phosphazene] (**11**) (Scheme 3). Although the synthesis of **11** was relatively straightforward, the purification proved to be difficult. Numerous reprecipitations into water or hexane followed by redissolution into pure THF brought about significant changes in the solubility of the polymer. It appears that peroxide formation from exposure of THF to atmospheric oxygen resulted in a partial oxidation of the thioether groups on the polymer to the sulfoxide, thus drastically changing the solubility properties. Furthermore, as indicated later by thermogravimetric analysis, **11** is not very stable thermally. The best conditions for purifying **11** without oxidation were by reprecipitation from chlorinated solvents, coupled with gravity filtration to remove sodium chloride.

Initially, the oxidation of **11** was attempted by a method similar to that used for the cyclic trimer **7**. Compound **11** was dissolved in chloroform to which was added H₂O₂ and H₂O (Scheme 3). The polymer initially precipitated from the chloroform solution but subsequently redissolved. The reaction product was poly[bis-(2-methylsulfoxyethoxy)phosphazene] (**12**).

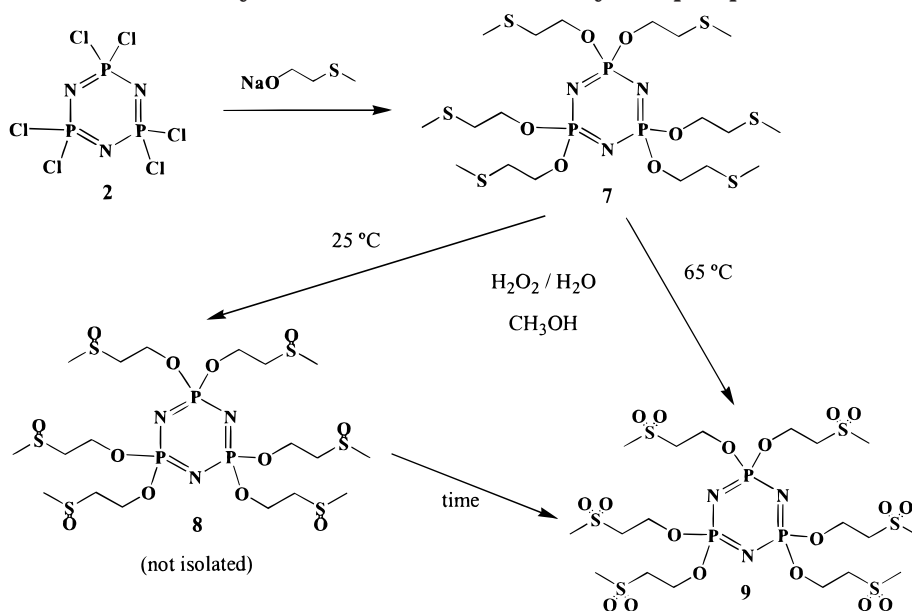
It became apparent that, for the synthesis of **12**, neither chloroform nor a pure sample of the thioether-bearing polymer **11** was necessary. The difficult purification of **11** was avoided. A solid, impure sample of **11** was oxidized by H₂O₂ in water. As the heterogeneous oxidation reaction proceeded, the polymer became soluble in the H₂O which was present. When the entire sample was completely dissolved in the water, the oxidation reaction of the thioether groups to the sulfoxide was complete.

Initially, solutions of **12** in water and H₂O₂ were heated to further oxidize the sulfur atom to the sulfone. This approach, although successful for the small-molecule model compounds, failed to result in complete conversion to the sulfone at the high polymeric phosphazene level. A more successful attempt involved the

Scheme 1. Synthesis of Pentaphenoxycyclotriphosphazenes



Scheme 2. Synthesis of Hexasubstituted Cyclotriphosphazenes



oxidation of **12** to poly[bis(2-methylsulfonylethoxy)phosphazene] (**13**) in the solid state with concentrated H_2O_2 (Scheme 3). Direct oxidation of **11** to **13** using *m*-chloroperoxybenzoic acid (MCPBA) was also performed successfully using a method similar to one used by Uranker et al. for oxidation of thioether-functionalized polystyrene.⁴³ Figure 2 shows the ^{13}C NMR spectra of compounds **11**–**13**.

Poly[bis(2-(2'-methylthioethoxy)ethoxy)phosphazene] (**14**), poly[bis(2-(2'-methylsulfoxyethoxy)ethoxy)phosphazene] (**15**), and poly[bis(2-(2'-methylsulfonylethoxy)ethoxy)phosphazene] (**16**) were also synthesized by the same techniques (Scheme 3). These polymers have an additional ethyleneoxy spacer group between the thioether, sulfoxide, or sulfone functional groups. Purification of **14** was easier than that for **11**. Polymer

14 could be oxidized by a dilute aqueous solution of H_2O_2 to form **15**. Species **16** was synthesized both by the oxidation of **15** by concentrated H_2O_2 in the solid state and also by oxidation of **14** by MCPBA.

Thermal Analysis. Glass Transition Temperatures. The thermal transitions of polymers **11**–**16** were measured by differential scanning calorimetry. None of the polymers showed evidence of crystallinity. However, a marked rise in glass transition temperature was detected with the increase in oxidation state of the sulfur atom on the pendent side group (Table 2).

The T_g increased from -73 to $+3$ $^\circ\text{C}$ following oxidation of the thioether group of polymer **11** to the sulfoxide group of polymer **12**. The T_g of **13**, which bears the sulfone group, is $+19$ $^\circ\text{C}$. This is a high value for an alkoxy-substituted polyphosphazene, although higher

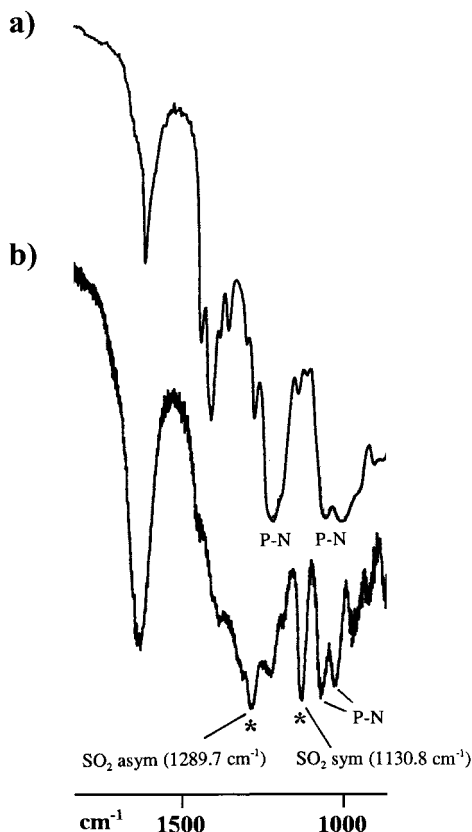
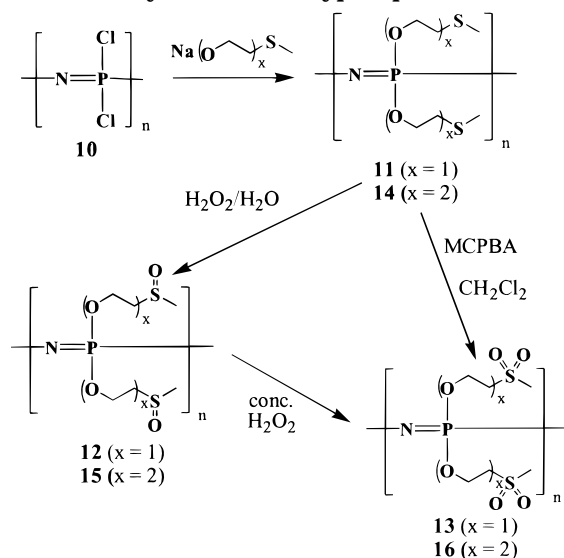


Figure 1. Infrared spectra of (a) thioether-bearing cyclic trimer **7** and (b) sulfone-bearing trimer **9**.

Scheme 3. Synthesis of Polyphosphazenes 11–16



values exist for certain adamantyl-substituted alkoxy polymers.⁴⁴ The high polarity of both the sulfoxide and sulfone functional groups causes dipolar association. This lowers polymer flexibility and results in an increased T_g . Polymers **14**–**16**, which contain an additional ethyleneoxy spacer unit, show a similar trend as the oxidation state of the sulfur atom is increased. However, the additional polymer flexibility offered by the ethyleneoxy spacer group gives lower T_g values for polymers **15** and **16**.

Thermal Stability. The thermogravimetric analysis (TGA) of polymers **11**–**13** (Table 2) gave similar results, with each showing a two-step decomposition process.

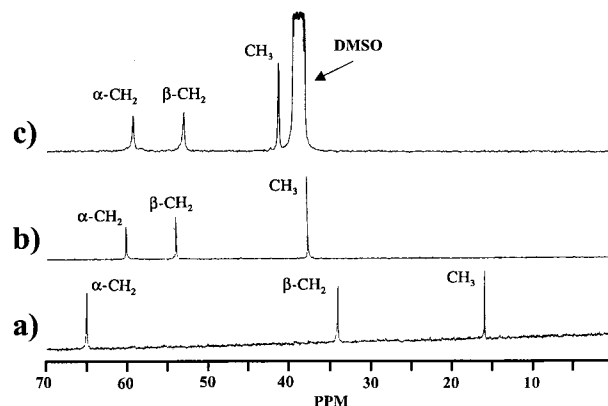


Figure 2. ^{13}C NMR spectra for (a) thioether-functionalized polymer **11**, (b) sulfoxide-functionalized polymer **12**, and (c) sulfone-functionalized polymer **13**.

Table 2. DSC and TGA Data for Polymers 11–16

polymer	DSC T_g (°C)	TGA		
		initial wt loss (°C)	secondary wt loss (°C)	char yield (%)
11	−73	169	335	26.4
12	3	224	566	21.1
13	19	256	636	12.2
14	−70			
15	−21			
16	−8			

The initial, significant weight loss at 169 °C detected for polymer **11** illustrated the thermal sensitivity of this material. However, the temperatures of both the initial and secondary weight losses increased as the oxidation state of the sulfur atom increased. Thus, oxidation of the sulfur atom may enhance the thermal stability of the polymer. The char yield at 900 °C reflects the proportion of **11**–**13** that consists of the phosphorus and nitrogen backbone.

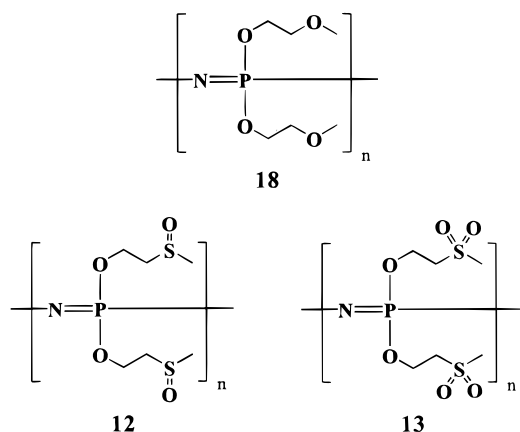
Ionic Conductivity. Solid Polymer Electrolytes.

Use of polymers **12**, **13**, **15**, and **16** as useful *solid* polymer electrolytes was precluded by their high glass transition temperatures. At ambient temperatures, these polymers do not have sufficient mobility to allow significant conduction of ions. Moreover, complexation with lithium salts would cause the glass transition temperatures to rise even more due to ionic cross-linking. Complexes of polymers **12** and **15** with LiSO_3CF_3 had conductivities below 10^{-8} S/cm, the lowest threshold that could be measured using our apparatus.

Gel Electrolyte Systems. A variety of crystalline or high T_g polymers have been used as host materials for gel–electrolyte systems. Conductivity in these systems is promoted by the presence of organic small molecules, such as propylene carbonate or *N*-methylpyrrolidone (NMP), which swell the polymer matrix. Often, interactions between the host polymer and the dissolved cations, in competition with solvent–ion interactions, will inhibit cation migration and diminish the conductivity. This competition between various polymers and the solvent for cation coordination has been studied through NMR, infrared, Raman, and fluorescence spectroscopy techniques.^{45,46} In this work, we used polymers with different coordination sites for conductivity studies in an attempt to understand the role of polymer–cation interactions in gel–electrolyte systems.

The polymers used as host materials were **12** and **13**, with sulfoxide and sulfone functional groups adjacent

to the methyl groups at the terminus of each side chain, and, for comparison, poly[bis(2-methoxyethoxy)phosphazene] (**18**), which contains an oxygen ether unit at



the same position. Each polymer was complexed with 5 wt % LiSO_3CF_3 and was then swollen with propylene carbonate (PC) in three different concentrations. The ionic conductivity of these polymer–salt–PC systems was measured over the temperature range 20–80 °C. Polymer **11**, the analogous species with the thioether functional group, was not used in this study because of its immiscibility with propylene carbonate.

The temperature dependence of conductivity has previously been described by the Arrhenius equation:⁴⁷

$$\sigma = \sigma_0 \exp(-E_A/kT)$$

where σ is the conductivity, T is the absolute temperature, σ_0 is the conductivity at some reference temperature, E_A is the activation energy, and k is Boltzmann's constant. For practical analysis, $\log(\sigma)$ is often plotted versus $1000/T$, a relationship which should be linear if the conductivity of the system follows Arrhenius behavior. The conductivity of systems such as liquid electrolytes is adequately described by the Arrhenius equation.

The Arrhenius equation has typically been insufficient to describe *solid polymer* electrolyte systems. Many Arrhenius plots of the conductivity of solid polymer electrolytes are curved rather than linear. It has been determined empirically that conductivity in solid polymer electrolytes is more accurately described by the Vogel–Tamman–Fulcher (VTF) equation:^{1,47–51}

$$\sigma = \sigma_0 \exp(-B/k(T - T_0))$$

where the conductivity σ is now related to a reduced temperature ($T - T_0$) in which the absolute temperature T is referenced to some arbitrary T_0 . VTF plots are constructed by plotting $\log(\sigma)$ versus $1000/(T - T_0)$. For polymer electrolyte systems, T_0 is often assumed to be the T_g .

The variable-temperature ionic conductivity of a complex of polymer **18** with 5 wt % LiSO_3CF_3 relative to the polymer (6.6 mol %) was measured with 0, 12.0, 35.3, and 53.1 wt % added propylene carbonate. An Arrhenius plot of the data (Figure 3) shows that the conductivity increases with an increasing concentration of propylene carbonate, despite the fact that this also follows a dilution of the number of Li^+ ions present. The Arrhenius plot of the complex of **18** without any added propylene carbonate shows almost no curvature. The

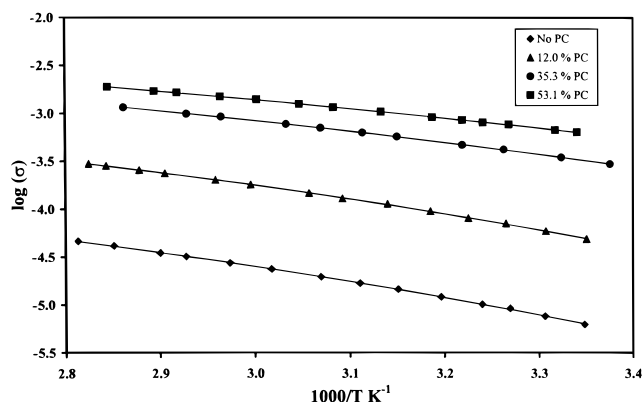


Figure 3. Arrhenius plots for polymer **18** complexed with 6.6 mol % LiSO_3CF_3 and mixed with propylene carbonate.

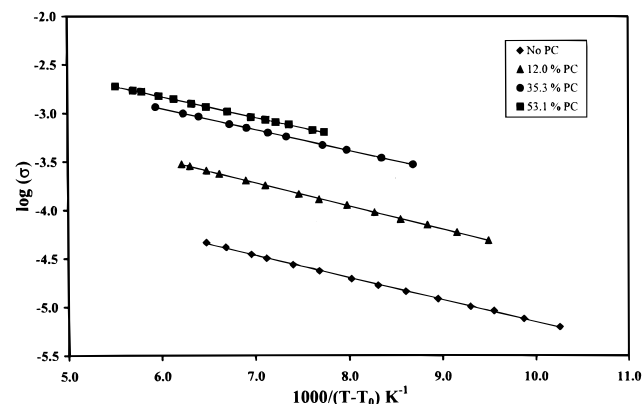


Figure 4. VTF plots for polymer **18** complexed with 6.6 mol % LiSO_3CF_3 and mixed with propylene carbonate. T_0 is assumed to be T_g .

data also fit VTF curves (Figure 4) very well, producing straight lines with T_0 assumed to be the T_g for each system.

Polymer **12** was complexed with 5 wt % LiSO_3CF_3 (8.7 mol %) and then swollen with 13.0, 33.9, and 51.7 wt % propylene carbonate. The ionic conductivities and glass transition temperatures of these mixtures, and a sample without solvent, were measured. The polymer–salt complex without solvent, with a glass transition temperature of +18 °C, showed no measurable ionic conductivity ($<10^{-8}$ S/cm) at ambient temperatures. Heating to 47.7 °C was required before meaningful data were obtained.

Figure 5 is an Arrhenius plot of the variable-temperature ionic conductivity of these systems. First, an increase in the propylene carbonate content increases the ionic conductivity. Furthermore, samples with little or no solvent generated curved lines that indicated non-Arrhenius temperature-dependent behavior, while those with higher concentrations of the solvent are significantly more linear and fit well with the Arrhenius model. This implies that the mechanism of conduction changes from polymer-dependent ion-transfer processes to solvent-mediated transfer with increasing propylene carbonate content.

However, these polymer systems are not sufficiently modeled by VTF theory. The conductivity rises more rapidly with an increase in temperature than the VTF model would predict, thus producing nonlinear fits to the data. The most logical explanation is that the assumption that the T_0 in the equation is the same as T_g is insufficient. It has been noted previously that the

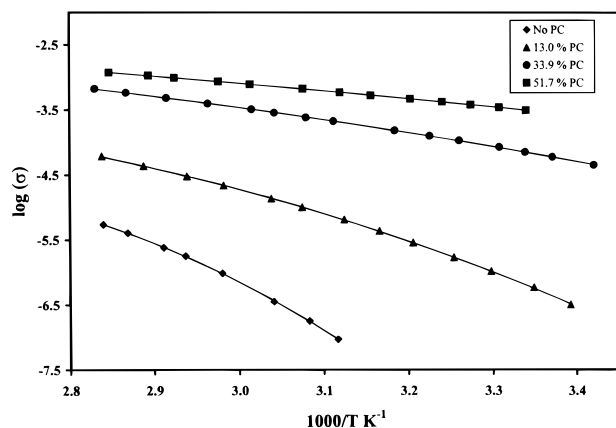


Figure 5. Arrhenius plots for polymer **12** complexed with 8.7 mol % LiSO_3CF_3 and mixed with propylene carbonate.

Table 3. Ionic Conductivity Data, Glass Transition Temperatures, and T_0 Values for Gel Systems Based on LiSO_3CF_3 Complexes with Polymers **18, **12**, and **13****

polymer	wt % PC	ionic conductivity, ^a σ (S/cm)			T_g (°C)	T_0^b
		25 °C	75 °C			
18	0	6.2×10^{-6}	3.9×10^{-5}		-72	T_g
18	12.0	4.9×10^{-5}	2.9×10^{-4}		-80	T_g
18	35.3	3.2×10^{-4}	1.1×10^{-3}		-92	T_g
18	53.1	6.2×10^{-4}	1.8×10^{-3}		-103	T_g
12	0	<i>c</i>	4.1×10^{-6}		18	$T_g - 50$
12	13.0	5.9×10^{-7}	5.0×10^{-5}		-14	$T_g - 45$
12	33.9	6.5×10^{-5}	5.8×10^{-4}		-33	$T_g - 35$
12	51.7	3.0×10^{-4}	1.1×10^{-3}		-40	$T_g - 30$
13	0	<i>d</i>	<i>d</i>		<i>d</i>	<i>d</i>
13	10.9	<i>c</i>	5.1×10^{-6}		8	$T_g - 80$
13	22.5	9.0×10^{-7}	4.0×10^{-5}		-20	$T_g - 60$
13	41.7	4.6×10^{-5}	2.0×10^{-4}		-40	$T_g - 55$

^a The conductivity values at these specific temperatures are approximate, interpolated from the data. ^b T_0 values used for fitting data to VTF curves. Indicated is whether T_g was used or, if not, how many degrees needed to be subtracted from T_g for the data to linearize. ^c The conductivity of this sample was below the lower limit of detection for our apparatus (10^{-8} S/cm). ^d This sample was not made.

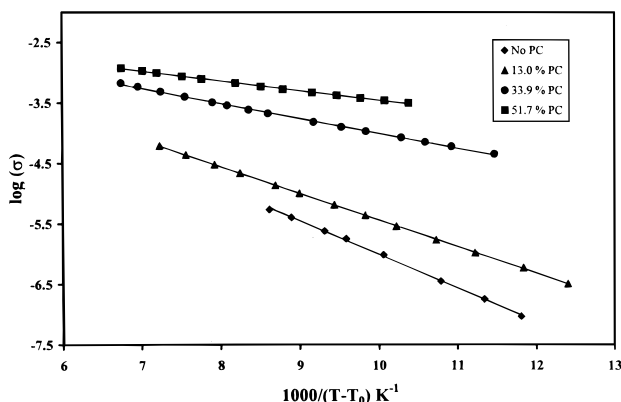


Figure 6. VTF plots for polymer **12** complexed with 8.7 mol % LiSO_3CF_3 and mixed with propylene carbonate. T_0 has been adjusted to linearize the data.

best fits of data to the VTF equation are sometimes given by T_0 values that are well below T_g .⁵² In fact, when T_0 is taken to be 30–50 K below T_g (Table 3), the data fit VTF theory very well (Figure 6). This indicates that the mechanism of conductivity is a very complicated process.

Previously Watanabe suggested that, for systems which display this type of temperature-dependent be-

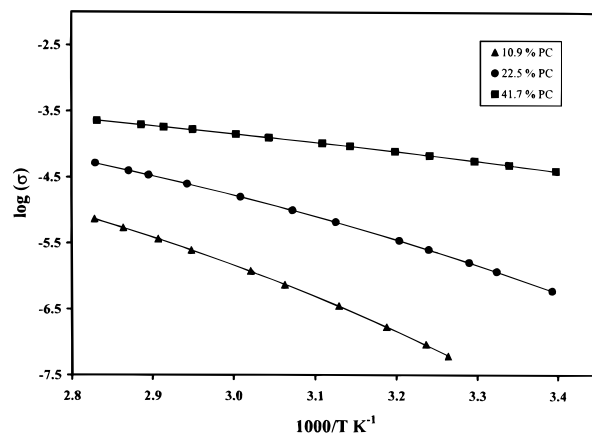


Figure 7. Arrhenius plots for polymer **13** complexed with 9.8 mol % LiSO_3CF_3 and mixed with propylene carbonate.

havior, the activation energy for movement of a cation with respect to the counterion or polymer host is not negligible.^{49,53–58} This indicates that the cation interacts strongly with either the anion or the host polymer. The segmental motion of the polymer is no longer the limiting characteristic of the ionic conductivity. In this system, with the highly polar sulfoxide groups, it can be assumed that the temperature-dependent behavior of ionic conductivity is evidence of strong cation–polymer interactions rather than a simple incomplete dissociation of salt. The increase in the glass transition temperature of polymer **12** after complexation with LiSO_3CF_3 confirms that the dissolved salts dissociate and coordinate to the polymer. VTF theory takes into account only the segmental motion of the polymer and assumes that cation–polymer interactions are negligible. The additional energy required to disrupt the interactions between the cation and the host is accounted for by choosing T_0 to be some value well below T_g . These interactions are then disrupted by the added propylene carbonate, and the ionic conductivity becomes a solvent-dependent process. The systems with higher concentrations of propylene carbonate required T_0 values with smaller shifts from T_g for the data to fit VTF theory.

Polymer **13** was mixed with 5 wt % LiSO_3CF_3 (9.8 mol %), swollen with 10.9, 22.5, and 41.7 wt % propylene carbonate, and allowed to stand for several weeks to allow for maximum homogenization of the ions and solvent through the samples. The ionic conductivities and glass transition temperatures of these mixtures were measured. A complex of the polymer with salt but without solvent was not made because polymer **13** is soluble only in highly polar, high-boiling solvents such as dimethyl sulfoxide (DMSO), which could not be removed completely from the polymer even after exposure to vacuum at 60 °C for 3 days. Because any residual solvent would bias the conductivity data, no further attempt was made to obtain a solid complex of this polymer with lithium triflate.

An Arrhenius plot of the variable-temperature conductivity data for systems based on polymer **13** showed results similar to those observed for polymer **12** (Figure 7). An increase in propylene carbonate content increases the ionic conductivity. Furthermore, all the lines were curved, indicating non-Arrhenius behavior, which became less obvious with increasing propylene carbonate content. Thus, polymer-mediated conduction of ions plays a greater role at lower concentrations of solvent.

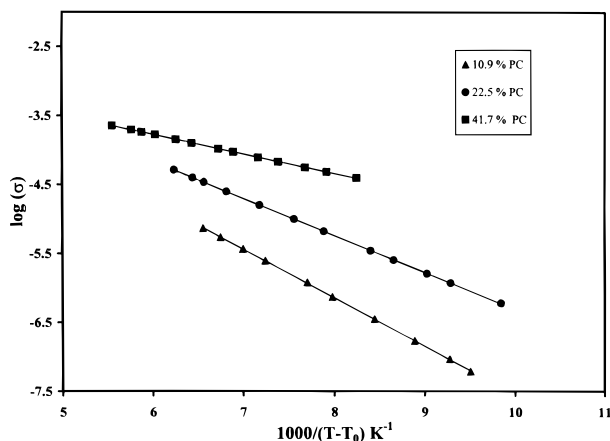


Figure 8. VTF plots for polymer **13** complexed with 9.8 mol % LiSO_3CF_3 and mixed with propylene carbonate. T_0 has been adjusted to linearize the data.

A VTF plot for the systems based on polymer **13** also generated a poor fit of data when T_0 is assumed to be the same as T_g . However, with T_0 taken as 55–80 K (Table 3) below T_g , an acceptable linear fit resulted (Figure 8). Once again, a more rapid rise occurred in conductivity with increasing temperature than predicted by VTF theory. Again, this necessitates the use of the reference temperature T_0 well below T_g . The strong interactions of the cation with the highly polar sulfone groups ensure that the conductivity is not limited solely by polymer segmental motion processes. There is a non-negligible activation energy for disruption of this coordination. The values of T_0 used for these complexes and gels involving polymer **13** are even further removed from T_g than the ones used for polymer **12**. This information, plus the ionic conductivity data, suggests that the sulfone groups of polymer **13** inhibit conductivity in the gel systems more significantly than do the sulfoxide groups of polymer **12**.

All the systems that used polymer **18**, with the ether terminal group, had higher ionic conductivities than polymer **12** (sulfoxide)- and **13** (sulfone)-based gels with comparable propylene carbonate concentrations. Polymer **12**-based gels had conductivities higher than those of polymer **13**-based counterparts (Table 3). For example, polymer **18**– LiSO_3CF_3 with 35.3 wt % propylene carbonate had a conductivity at 25 °C of approximately 3.2×10^{-4} S/cm. This is higher than the 6.5×10^{-5} S/cm value measured at 25 °C for a sample of polymer **12**– LiSO_3CF_3 with 33.9 wt % propylene carbonate. This in turn is higher than the 25 °C conductivity of 4.6×10^{-5} S/cm measured for polymer **13**– LiSO_3CF_3 with 41.7% propylene carbonate. The data for the conductivity at 75 °C show a similar trend. Highly polar functional groups on the host polymer in a gel–electrolyte system compete effectively with the added solvent molecules for interactions with lithium cations and thus reduce the conductivity. Thus, the conductivity in solvent-swollen systems that utilize host polymers **18**, **12**, and **13** decreased with increasing polarity of the functionality of the side group, in the order $\text{OCH}_3 > \text{S(O)CH}_3 > \text{S(O)}_2\text{CH}_3$.

This is in spite of the fact that the molar concentration of Li^+ was the lowest for polymer **18** and the highest for polymer **13** (although the *weight* concentration of LiSO_3CF_3 was the same for all systems). In *solid* polymer electrolytes, an increase in salt can yield lower ionic conductivities above a certain threshold value

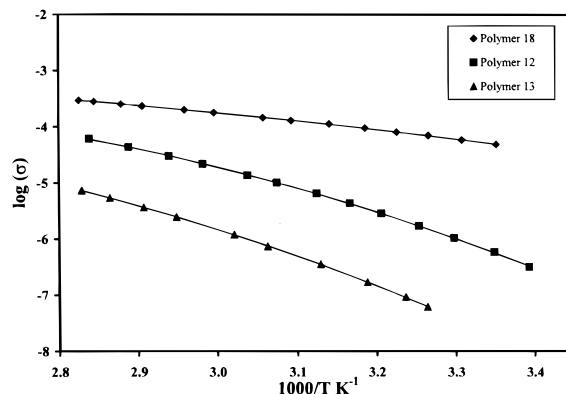


Figure 9. Arrhenius plots for LiSO_3CF_3 complexes of polymer **18** with 12.0 wt % propylene carbonate (PC), polymer **12** with 13% PC, and polymer **13** with 10.9 wt % PC.

because of coordinative cross-linking. When solvent is present, there are fewer coordinative cross-links and this salt concentration threshold is raised. In general, ionic conductivity in pure propylene carbonate increases with increasing salt concentration. Thus, at such low concentrations of salt, in solvent–polymer–salt systems, especially in the systems with significant amounts of propylene carbonate, the addition of more dissolved salts will result in a higher ionic conductivity.

Figure 9 is an Arrhenius plot of comparable propylene carbonate systems that utilize different polymer hosts: polymer **18** (ether) with 12.0 wt % propylene carbonate, polymer **12** (sulfoxide) with 13.0 wt % propylene carbonate, and polymer **13** (sulfone) with 10.9 wt % propylene carbonate. It can be seen that the sulfone- and sulfoxide-bearing polymers contribute to a greater deviation from Arrhenius-type behavior than that for the ether-bearing polymer. Thus, for those two systems, the polymer plays a far greater role in controlling transport of ions.

These data suggest that polymer host materials with strongly polar functional groups such as sulfoxides and sulfones compete more effectively against the added solvent molecules in gel–electrolytes for ion interactions. Interactions between the ions and the polymer matrix decrease conductivity and make ion transport more reliant on polymer-dependent processes than on the mobility of the solvent molecules.

Conclusions

Phosphazene trimers and polymers containing sulfone and sulfoxide functional groups have been synthesized. Phosphazene trimers bearing thioether functional groups were synthesized and subsequently oxidized to the sulfone, passing through a difficult-to-isolate sulfoxide intermediate. At the high polymer level, the oxidation of the sulfur atom by H_2O_2 is easily interrupted to yield a polymer fully functionalized with sulfoxide groups without overoxidation to the sulfone. The analogous polymer with sulfone functional groups can be obtained by continued oxidation of a sulfoxide-bearing polymer by concentrated H_2O_2 or by oxidation of the thioether via *m*-chloroperbenzoic acid (MCPBA). Oxidation of the sulfur atom raises the glass transition temperature due to the highly polar nature of sulfone and sulfoxide functional units.

The near-ambient-temperature glass transition temperatures of these polymers preclude their direct use as *solid* polymer electrolytes in most devices. However,

the polymers bearing ether, sulfoxide, and sulfone functional groups were studied as possible host matrixes for *gel-electrolyte* systems with propylene carbonate added as a solvent/plasticizer. Increased ionic conductivity with Arrhenius behavior occurred in all systems in the presence of the higher concentrations of propylene carbonate. The conductivity was decreased, and non-Arrhenius temperature-dependent behavior was observed, for host polymers that contained the strongly polar sulfone and sulfoxide groups. The sulfone group interferes more strongly with ion transport in the gel systems than does the sulfoxide group. Both systems required additional data manipulation in order to sufficiently fit the VTF model. This suggested that there is a non-negligible activation energy for dissociation of the lithium cation from the polymer, even in the presence of propylene carbonate, and polymer segmental motion is not the limiting factor for the conduction of ions.

Experimental Section

Equipment. High-field ^{31}P (146 MHz), ^{13}C (90 MHz), and ^1H (360 MHz) NMR spectra were obtained by using a Bruker WM360 spectrometer. Both ^{31}P and ^{13}C NMR spectra were proton decoupled. ^{31}P NMR spectra were referenced to external 85% H_3PO_4 with positive shifts recorded downfield of the reference. ^1H and ^{13}C NMR spectra were referenced to external tetramethylsilane. Positive-ion fast atom bombardment (FAB) mass spectroscopy was performed using a Kratos MS-50 mass spectrometer with a magnetic sector using xenon atoms. Infrared spectroscopy was performed using a Perkin-Elmer 1600 Series Fourier transform infrared spectrophotometer. Glass transition temperatures were determined by differential scanning calorimetry (DSC) using a Perkin-Elmer 7 thermal analysis system equipped with a Perkin-Elmer 7500 computer. All polymer samples were heated from at least -100 to $+60$ $^{\circ}\text{C}$. Some samples were heated to 150 $^{\circ}\text{C}$. Heating rates of 10, 20, and 40 $^{\circ}\text{C}/\text{min}$ were used, and the glass transition temperatures were determined by extrapolation to a heating rate of zero. Sample sizes were between 10 and 30 mg. Thermogravimetric analysis (TGA) was performed using a Perkin-Elmer 7 thermal analysis system using a heating rate of 10 $^{\circ}\text{C}/\text{min}$ from 25 to 900 $^{\circ}\text{C}$ under an atmosphere of nitrogen. Molecular weights of some polymers were estimated through the use of a Hewlett-Packard 1090 gel permeation chromatograph equipped with an HP 1047A refractive index detector. A 0.01 M solution of tetrabutylammonium nitrate in THF was used as the eluting solvent for two PhenomineX Phemgel linear 10 columns calibrated versus polystyrene standards. A 0.01 M solution of sodium azide in H_2O was used as the eluting solvent for Polymer Laboratories Aquagel columns calibrated versus poly(ethylene oxide) standards. Conductivity measurements were made using a Hewlett-Packard 4192A LF impedance analyzer with an ac frequency range of 5 Hz to 1 MHz and an oscillating potential of 0.1 V. Heating tape and a thermocouple threaded inside the Teflon impedance analysis fixture were used to control and measure the temperature for the variable-temperature experiments. All conductivity measurements were carried out in an argon-filled drybox. The dialysis purifications were carried out with the use of Spectra/Por 2 membranes with cutoffs of $12\,000$ to $14\,000$ MW.

Materials. Hexachlorocyclotriphosphazene (**2**) (Ethyl Corporation/Nippon Fine Chemical) was purified by recrystallization from hot heptane followed by sublimation at 40 $^{\circ}\text{C}$ (0.05 Torr). Poly(dichlorophosphazene) (**10**) was prepared by the thermal ring-opening polymerization of **2** in the melt at 250 $^{\circ}\text{C}$, as reported previously.⁵⁹ Tetrahydrofuran (THF) was dried over sodium benzophenone ketyl and was distilled in an atmosphere of dry argon before use. 2-(Methylsulfonyl)ethanol, 2-(methylthio)ethanol, 2-methoxyethanol, and 2-(2'-methoxyethoxy)ethanol (Aldrich) were distilled from CaH_2 onto

molecular sieves within 24 h prior to use. Poly[bis(2-(2'-methoxyethoxy)ethoxy)phosphazene] (**1**),⁶⁰ $\text{N}_3\text{P}_3(\text{OC}_6\text{H}_5)_5\text{Cl}$ (**3**),⁶¹ and poly[bis(2-methoxyethoxy)phosphazene] (**18**)⁸ were synthesized as reported previously. Lithium triflate (Aldrich) was dried under vacuum and was stored in an argon-filled drybox before use. Anhydrous propylene carbonate (Aldrich) was stored in an argon-filled drybox before use. All other reagents were used as received. Reactions that involved the use of chlorophosphazenes were carried out under an atmosphere of dry argon.

Reaction of $\text{N}_3\text{P}_3\text{Cl}_6$ (2**) with $\text{NaOCH}_2\text{CH}_2\text{S}(\text{O})_2\text{CH}_3$.** A solution of 2-(methylsulfonyl)ethanol (Aldrich) (2.5 g, 0.020 mol) in THF (25 mL) was added via cannula to a suspension of sodium hydride (0.82 g of a 60% emulsion in mineral oil, 0.021 mol) in THF (100 mL). The sodium salt formed precipitated from solution and was kept in suspension as a slurry with vigorous stirring. A solution of $\text{N}_3\text{P}_3\text{Cl}_6$ (**2**) (1.0 g, 0.0029 mol) in THF (50 mL) was added dropwise via addition funnel. The reaction mixture was stirred for 24 h at room temperature. Two soluble intermediate species were detected by ^{31}P NMR, but precipitation of the final product caused disappearance of the phosphorus signal. The solvents were removed by rotary evaporation to leave a brown powdery product which was soluble in D_2O .

^{31}P NMR Data. Intermediate A (in THF): AB_2 δ (ppm) 17.8 (d), -4.7 (t). Intermediate B (in THF): AB_2 δ (ppm) 20.0 (d), -10.7 (t). Product (in D_2O): δ (ppm) -1.0 (s).

Reaction of $\text{N}_3\text{P}_3(\text{OC}_6\text{H}_5)_5\text{Cl}$ (3**) with $\text{NaOCH}_2\text{CH}_2\text{S}(\text{O})_2\text{CH}_3$.** This reaction was carried out in a manner similar to that for the preceding experiment. The reagents and quantities used were 2-(methylsulfonyl)ethanol (0.23 g, 0.0019 mol) in THF (25 mL), sodium hydride (0.10 g of a 60% emulsion in mineral oil, 0.0025 mol) in THF (100 mL), and $\text{N}_3\text{P}_3(\text{OC}_6\text{H}_5)_5\text{Cl}$ (**3**) (1.0 g, 0.0016 mol) in THF (50 mL). ^{31}P NMR detected only one reaction product. ^{31}P NMR (THF): AB_2 δ (ppm) 10.0 (d), 6.2 (t). FAB mass spectrometry (m/e): 662 MH^+ .

$\text{N}_3\text{P}_3(\text{OC}_6\text{H}_5)_5(\text{OCH}_2\text{CH}_2\text{SCH}_3)$ (4**).** 2-(Methylthio)ethanol (Aldrich) (0.85 g, 0.0092 mol) was added via syringe to a suspension of sodium hydride (0.35 g of a 60% emulsion in mineral oil, 0.00875 mol) in THF (50 mL), and the mixture was stirred for 4 h. A solution of **3** (5.10 g, 0.00802 mol) in THF (40 mL) was added dropwise via syringe. The reaction was stirred at room temperature for 24 h. After the substitution was complete, the reaction mixture was filtered and solvents were removed by rotary evaporation. The residue was dissolved in methylene chloride (100 mL) and washed with distilled, deionized water (3×50 mL). The aqueous layer was extracted once with CH_2Cl_2 . The combined organic fractions were dried with MgSO_4 and filtered, and the solvent was evaporated. The residue was passed through a short silica column (3 cm diameter \times 5 cm length of 80 – 250 mesh silica gel) with a $50/50$ CH_2Cl_2 /hexane mixture used as the mobile phase. The recovered oily residue was washed thoroughly with hexane, and the solvents were allowed to evaporate to yield **4** (3.9 g, 70%). ^1H NMR (CDCl_3): δ (ppm) 2.0 (s, 3H, CH_3S), 2.45 (t, 2H, CH_2S), 3.65 (m, 2H, OCH_2), 6.9 (m, 5H, Ar), 7.1 – 7.3 (m, 20H, Ar). ^{13}C NMR (CDCl_3): δ (ppm) 15.9 (CH_3S), 33.3 (CH_2S), 65.4 (OCH_2), 120.9 , 121.0 , 124.9 , 125.1 , 129.5 , 150.6 (all Ar). ^{31}P NMR (CDCl_3): AB_2 δ (ppm) 9.7 (dd, PRR'), 13.1 (dt, PR₂), $J_{\text{PP}} = 79.1$. FAB mass spectrometry (m/e): 692 , MH^+ , base peak.

$\text{N}_3\text{P}_3(\text{OC}_6\text{H}_5)_5(\text{OCH}_2\text{CH}_2\text{S}(\text{O})\text{CH}_3)$ (5**) and $\text{N}_3\text{P}_3(\text{OC}_6\text{H}_5)_5(\text{OCH}_2\text{CH}_2\text{S}(\text{O})_2\text{CH}_3)$ (**6**).** Potassium peroxydisulfate (Oxone, $2\text{KHSO}_5 \cdot \text{K}_2\text{SO}_4 \cdot \text{KHSO}_4$) was used as the oxidizing agent, according to a technique previously reported.⁴² Wet alumina was prepared by mixing 1 g of H_2O with 5 g of 80 – 200 mesh Brockmann I grade neutral alumina (Fischer) and shaking until the mixture was a uniform, smooth-flowing powder. To a slurry of wet alumina (1.0 g) and Oxone (Acros) (1.34 g, 0.00218 mol) in chloroform (10 mL) was added a solution of **4** (1.03 g, 0.00149 mol) in chloroform (5 mL). The mixture was refluxed for 2.5 h, after which time the mixture was filtered and the solids were washed thoroughly with CHCl_3 . The solvents were then removed by rotary evaporation. ^1H NMR indicated 35% **5** and 65% **6**. The product residue was then

redissolved in CHCl_3 (10 mL) and added to a slurry of wet alumina (1.0 g) and Oxone (0.50 g, 0.00081 mol) in CHCl_3 , and the resulting mixture was refluxed for an additional 5 h. The mixture was filtered, the solids were washed thoroughly with CHCl_3 , and the solvent was removed by rotary evaporation. ^1H NMR indicated the presence of **6** (100%).

Characterization Data for 5. ^1H NMR (CDCl_3): δ (ppm) 2.4 (s, $\text{CH}_3\text{S}(\text{O})$), 2.6–2.8 (br, $\text{CH}_2\text{S}(\text{O})$), 3.7–3.9 (br, OCH_2), 6.9–7.4 (m, br, Ar). ^{13}C NMR (CDCl_3): δ (ppm) 39.0 ($\text{CH}_3\text{S}(\text{O})$), 54.6 ($\text{CH}_2\text{S}(\text{O})$), 58.9 (OCH_2) (120–150, several aromatic peaks which overlap with those of **6**). ^{31}P NMR (CDCl_3): AB_2 δ (ppm) 9.6 (dd, PRR'), 13.4 (dt, PR_2), $J_{\text{PP}} = 80.7$. FAB mass spectrometry (m/e): 708 MH^+ base peak.

Characterization Data for 6. ^1H NMR (CDCl_3): δ (ppm) 2.7 (s, 3H, $\text{CH}_3\text{S}(\text{O})_2$), 2.9 (t, 2H, $\text{CH}_2\text{S}(\text{O})_2$), 3.85 (m, 2H, OCH_2), 6.9 (m, 5H, Ar), 7.1–7.3 (m, 20H, Ar). ^{13}C NMR (CDCl_3): δ (ppm) 42.4 ($\text{CH}_3\text{S}(\text{O})_2$), 55.1 ($\text{CH}_2\text{S}(\text{O})_2$), 60.0 (OCH_2), 120.9, 121.2, 125.0, 125.3, 129.5, 150.6 (all Ar). ^{31}P NMR (CDCl_3): AB_2 δ (ppm) 9.6 (dd, PRR'), 13.4 (dt, PR_2), $J_{\text{PP}} = 80.6$. FAB mass spectrometry (m/e): 724 MH^+ base peak.

Hexakis(2-methylthioethoxy)cyclotriphosphazene (7). 2-(Methylthio)ethanol (10.8 g, 0.117 mol) (Aldrich) was added via syringe to sodium metal (2.61 g, 0.114 mol) in THF (300 mL). After all the sodium had reacted, a solution of **2** (6.00 g, 0.0173 mol) was added dropwise via syringe. The reaction mixture was stirred at ambient temperature for 48 h. After the substitution was complete, the solvents were removed by rotary evaporation and the residue was dissolved in CH_2Cl_2 and washed with distilled, deionized water (4×75 mL). The aqueous washings were extracted with CH_2Cl_2 . The combined organic layers were then dried with MgSO_4 and filtered, and the solvent was allowed to evaporate. The oily residue was washed thoroughly with hexanes, and the residue was allowed to dry. ^1H NMR indicated no residual alcohols. **7** was recovered as a yellow oil (7.47 g, 64%). ^1H NMR (CDCl_3): δ (ppm) 2.2 (s, 3H, CH_3S), 2.8 (t, 2H, CH_2S), 4.3 (m, 2H, OCH_2). ^{13}C NMR (CDCl_3): δ (ppm) 15.9 (CH_3S), 33.7 (CH_2S), 65.1 (OCH_2). ^{31}P NMR (CDCl_3): δ (ppm) 17.9 (s). FAB mass spectrometry (m/e): 682 MH^+ base peak. IR (cm^{-1}): 1227.4 (P–N stretch).

Hexakis(2-(methylsulfoxy)ethoxy)cyclotriphosphazene (8) and Hexakis(2-(methylsulfonyl)ethoxy)cyclotriphosphazene (9). Compound **8** was not isolated but was detected briefly as an intermediate before conversion to **9**. Species **7** (0.20 g, 0.000 29 mol) was dissolved in methanol (0.5 mL), to which was added 35% H_2O_2 (0.5 g) (Acros) in water. The product precipitated from solution after the addition of the peroxide but then subsequently redissolved in the reaction mixture. Methanol (1 mL) and distilled, deionized water (2 mL) were added. The reaction mixture was stirred without a cover for 24 h, during which time the solvents evaporated. ^1H and ^{13}C NMR indicated that **8** was the only product. Within 24 h **8** was converted to **9**.

Compound **9** was produced directly via a similar procedure. Species **7** (0.20 g, 0.000 29 mol) was dissolved in methanol (2 mL), to which was added 35% H_2O_2 (0.5 mL, 0.0057 mol). The mixture was warmed at 65 °C for 5 h, after which time the solvents were removed by rotary evaporation. ^1H and ^{13}C NMR confirmed the conversion of **7** to **9**. Although **9** was initially soluble in water, methanol, and chloroform, after thorough drying under vacuum it was soluble only in DMSO, acetonitrile/methanol mixtures, and NMP. It was recovered as a white powder which was washed thoroughly with water to remove excess H_2O_2 . The NMR data given here were obtained in D_2O , before this final purification step.

Characterization Data for 8. ^1H NMR (D_2O): δ (ppm) 2.65–2.75 (br, 3H, $\text{CH}_3\text{S}(\text{O})$), 3.05–3.2 (br, 1H, $\text{CHH}'\text{S}(\text{O})$), 3.2–3.35 (br, 1H, $\text{CHH}'\text{S}(\text{O})$), 4.2–4.5 (br, overlaps with D_2O , OCH_2). ^{13}C NMR (D_2O): δ (ppm) 37.4 ($\text{CH}_3\text{S}(\text{O})$), 53.4 ($\text{CH}_2\text{S}(\text{O})$), 60.4 (OCH_2). ^{31}P NMR (D_2O): δ (ppm) 16.8 (s).

Characterization Data for 9. ^1H NMR (D_2O): δ (ppm) 3.0 (s, 3H, $\text{CH}_3\text{S}(\text{O})_2$), 3.5 (t, 2H, $\text{CH}_2\text{S}(\text{O})_2$), 4.3 (m, 2H, OCH_2). ^{13}C NMR (D_2O): δ (ppm) 42.1 ($\text{CH}_3\text{S}(\text{O})_2$), 54.0 ($\text{CH}_2\text{S}(\text{O})_2$), 60.6 (OCH_2). ^{31}P NMR (D_2O): δ (ppm) 16.7 (s). FAB mass spectrometry (m/e): 874 MH^+ , 792 $\text{M}(\text{S}(\text{O})_2\text{CH}_3)_2\text{H}_2^+$, 768

$\text{M}(\text{CH}_2\text{CH}_2\text{S}(\text{O})_2\text{CH}_3)_2\text{H}_2^+$, 690 $\text{M}(\text{CH}_2\text{CH}_2\text{S}(\text{O})_2\text{CH}_3)(\text{S}(\text{O})_2\text{CH}_3)_3^+$, 662 $\text{M}(\text{CH}_2\text{CH}_2\text{S}(\text{O})_2\text{CH}_3)_3^+$, 584 $\text{M}(\text{CH}_2\text{CH}_2\text{S}(\text{O})_2\text{CH}_3)(\text{S}(\text{O})_2\text{CH}_3)_4^+$, 556 $\text{M}(\text{CH}_2\text{CH}_2\text{S}(\text{O})_2\text{CH}_3)_4^+$ base peak, 478 $\text{M}(\text{CH}_2\text{CH}_2\text{S}(\text{O})_2\text{CH}_3)(\text{S}(\text{O})_2\text{CH}_3)_5^+$, 450 $\text{M}(\text{CH}_2\text{CH}_2\text{S}(\text{O})_2\text{CH}_3)_5^+$. IR (cm^{-1}): 1289.7 (asymmetric O=S=O stretch), 1228.0 (P–N stretch), 1130.8 (symmetric O=S=O stretch).

Poly[bis(2-(methylthio)ethoxy)phosphazene] (11). 2-(Methylthio)ethanol (4.0 g, 0.043 mol) (Aldrich) was added via syringe to a suspension of sodium hydride (1.8 g of a 60% emulsion in mineral oil, 0.045 mol) in THF (200 mL), and the mixture was stirred for 16 h. A solution of poly(dichlorophosphazene) (**10**) (2.0 g, 0.017 mol) in THF (150 mL) was then added dropwise via cannula. The mixture was stirred at room temperature for 48 h. After the substitution was complete, THF stabilized with 25 ppm butylated hydroxytoluene (100 mL) was added. The mixture was concentrated by rotary evaporation and precipitation into distilled, deionized water. The recovered polymer was dissolved in methylene chloride, filtered to remove salts, and precipitated into hexanes. This was repeated numerous times. The final product, **11**, was recovered as a yellow solid (4.9 g, 63%). Polymer **11** was soluble in DMF, THF, and chlorinated solvents. ^1H NMR (CDCl_3): δ (ppm) 2.2 (br, 3H, CH_3S), 2.8 (br, 2H, CH_2S), 4.1 (br, 2H, OCH_2). ^{13}C NMR (CDCl_3): δ (ppm) 16.0 (CH_3S), 34.1 (CH_2S), 65.0 (OCH_2). ^{31}P NMR (CDCl_3): δ (ppm) –7.4 (s). GPC (THF): $M_w = 2.3 \times 10^5$, PDI = 2.5.

Poly[bis(2-(methylsulfoxy)ethoxy)phosphazene] (12). To a solid, impure sample of **11** (5.0 g, ~0.22 mol) was added 35% H_2O_2 (40 mL, 0.46 mol). This was diluted with water (400 mL). The mixture was stirred for 24 h, at which point the polymer was completely dissolved. The polymer was dialyzed in water (10 days) and methanol (4 days). The solvents were then removed, and the polymer was recovered as a yellow solid (3.1 g, 55%). Polymer **12** was soluble in water, methanol, and DMSO. ^1H NMR (D_2O): δ (ppm) 2.7 (br, 3H, $\text{CH}_3\text{S}(\text{O})$), 3.1 (br, 1H, $\text{CHH}'\text{S}(\text{O})$), 3.2 (br, 1H, $\text{CHH}'\text{S}(\text{O})$), 4.4–4.5 (d, 2H, OCH_2). ^{13}C NMR (D_2O): δ (ppm) 37.8 ($\text{CH}_3\text{S}(\text{O})$), 54.1 ($\text{CH}_2\text{S}(\text{O})$), 60.2 (OCH_2). ^{31}P NMR (D_2O): δ (ppm) –6.5 (s). GPC (H_2O): $M_w = 5.5 \times 10^5$, PDI = 12.3.

Poly[bis(2-(methylsulfonyl)ethoxy)phosphazene] (13). **Via H_2O_2 .** Polymer **12** (purified) (1.33 g, 0.00585 mol) was dissolved in methanol (15 mL), and 35% H_2O_2 (1 mL, 0.011 mol) was added to this solution. The solvents and water were then removed by rotary evaporation. The solid residue was stored for 48 h, after which time it was water insoluble. It was then washed repeatedly with water and methanol to remove excess H_2O_2 . Polymer **13** was recovered as a white solid (0.89 g, 52%).

Via MCPBA. A solution of polymer **11** (0.51 g, 0.00224 mol) in CHCl_3 (30 mL) was cooled to 0 °C in an ice water bath. To this was added MCPBA (3.5 g, 0.020 mol) (Aldrich). The mixture was stirred for 15 min, after which the ice bath was removed and the solution was allowed to warm to room temperature. After 16 h at 25 °C, the solvents were removed by rotary evaporation and the solid residue was washed repeatedly with methanol. The solid residue recovered was polymer **13** (0.59 g, 90%). Polymer **13** was soluble in DMSO and DMF. ^1H NMR ($\text{DMSO}-d_6$): δ (ppm) 3.1 (br, 3H, $\text{CH}_3\text{S}(\text{O})_2$), 3.5 (br, 2H, $\text{CH}_2\text{S}(\text{O})_2$), 4.3 (br, 2H, OCH_2). ^{13}C NMR ($\text{DMSO}-d_6$): δ (ppm) 42.1 ($\text{CH}_3\text{S}(\text{O})_2$), 53.9 ($\text{CH}_2\text{S}(\text{O})_2$), 60.1 (OCH_2). ^{31}P NMR ($\text{DMSO}-d_6$): δ (ppm) –7.3 (s).

Poly[bis(2-(2'-(methylthio)ethoxy)ethoxy)phosphazene] (14). Polymer **14** was synthesized by a method similar to that for the preparation of **11**. The reagents and quantities used were compound **17** (9.2 g, 0.068 mol), sodium metal (1.5 g, 0.066 mol), and polydichlorophosphazene (**10**) (1.3 g, 0.011

mol). Polymer **14** was purified by multiple reprecipitations from THF into water, methanol, and hexane (2.6 g, 74%). Polymer **14** was soluble in THF and chlorinated solvents. ^1H NMR (CDCl_3): δ (ppm) 2.1 (br, 3H, CH_3S), 2.7 (t, 2H, CH_2S), 3.5–3.7 (m, 4H, CH_2OCH_2), 4.1 (br, 2H, POCH_2). ^{13}C NMR (CDCl_3): δ (ppm) 16.1 (CH_3S), 33.6 (CH_2S), 65.0 (POCH_2), 70.2, 70.5. ^{31}P NMR (CDCl_3): δ (ppm) –7.7 (s). GPC (THF): $M_w = 2.3 \times 10^5$.

Poly[bis(2-(2'-(methylsulfoxy)ethoxy)ethoxy)phosphazene] (15). Polymer **15** was prepared by a method similar to that for the synthesis of **12**. The reagents and quantities used were polymer **14** (0.25 g, 0.00079 mol), 35% H_2O_2 (1.5 mL, 0.017 mol), and additional water (5 mL). Polymer **15** was purified by dialysis (0.21 g, 77%). Polymer **15** was soluble in water, methanol, and chlorinated solvents. ^1H NMR (CDCl_3): δ (ppm) 2.65 (s, 3H, CH_3S), 2.9 (m, 1H, $\text{CHH}'\text{S}$), 3.1 (m, 1H, $\text{CHH}'\text{S}$), 3.7 (t, 2H), 3.9 (t, 2H), 4.1 (br, 2H, POCH_2). ^{13}C NMR (CDCl_3): δ (ppm) 39.3 (CH_3S), 54.6 ($\text{CH}_2\text{S}(\text{O})$), 63.7, 65.0, 70.4. ^{31}P NMR (CDCl_3): δ (ppm) –7.9 (s).

Poly[bis(2-(2'-(methylsulfonyl)ethoxy)ethoxy)phosphazene] (16). Via H_2O_2 . Polymer **16** was obtained by a method similar to that for the synthesis of **13**. The reagents and quantities used were polymer **15** (0.25 g, 0.00072 mol), 35% H_2O_2 (1 mL, 0.001 mol), and water (5 mL). Polymer **16** was purified by washing with water and methanol.

Via MCPBA. Polymer **16** was prepared by a process similar to that described for **13**. The reagents and quantities used were polymer **14** (0.5 g, 0.0016 mol), MCPBA (3.5 mL, 0.020 mol), and CHCl_3 (5 mL). Polymer **16** was purified by washing thoroughly with methanol (0.48 g, 80%). Polymer **16** was soluble in DMSO. ^1H NMR ($\text{DMSO}-d_6$): δ (ppm) 3.0 (s, 3H, $\text{CH}_3\text{S}(\text{O})_2$), 3.4 (br, 2H, $\text{CH}_2\text{S}(\text{O})_2$), 3.6 (br, 2H), 3.8 (br, 2H), 4.0 (br, 2H, POCH_2). ^{13}C NMR ($\text{DMSO}-d_6$): δ (ppm) 42.1 ($\text{CH}_3\text{S}(\text{O})_2$), 53.8 ($\text{CH}_2\text{S}(\text{O})_2$), 64.2, 64.5, 69.4. ^{31}P NMR ($\text{DMSO}-d_6$): δ (ppm) –7.9 (s).

2-(2'-(Methylthio)ethoxy)ethanol (17). A reaction flask containing sodium methanethiolate (10 g, 0.14 mol) (Fluka) in dry dioxane (400 mL) was warmed gently. To this warm solution was added 2-(2'-(chloroethoxy)ethanol (11.88 g, 0.095 mol) (Aldrich) over a period of 1 h. The reaction mixture was stirred and heated at reflux for 12 h. After this time, the mixture was cooled to ambient temperature, and distilled water (100 mL) was added to dissolve the salts formed. The solution was extracted four times with chloroform. The organic fractions were combined and dried with MgSO_4 . The drying agent was filtered off, and the solvent was removed by rotary evaporation. A pale, yellow oil remained, which was distilled under reduced pressure (70–75 °C, 0.05 mmHg) to yield a clear, colorless liquid (10.6 g, 82%). ^1H NMR (CDCl_3): δ (ppm) 2.1 (s, 3H, CH_3S), 2.4 (t, 1H, OH), 2.7 (t, 2H, CH_2S), 3.6 (t, 2H), 3.7 (m, 4H). ^{13}C NMR (CDCl_3): δ (ppm) 16.0 (CH_3S), 33.7 (CH_2S), 61.7, 70.0, 72.0. CI mass spectrometry (m/e): 137 MH^+ base peak.

Acknowledgment. We thank the Department of Energy (Grant No. DE-FG02-93ER14387), the National Science Foundation, and the Electric Power Research Institute for their financial support. We also thank Dr. Digby D. Macdonald for many valuable discussions.

References and Notes

- Armand, M. B.; Chabagno, J. M.; Duclot, M. J. Second International Conference on Solid Electrolytes, St. Andrews, Scotland, 1978.
- Armand, M. B.; Chabagno, J. M.; Duclot, M. J. In *Fast Ion Transport in Solids*; Duclot, M. J., Vashishta, P., Mundy, J. N., Shenoy, G. K., Eds.; North-Holland: Amsterdam, 1979.
- Fenton, D. E.; Parker, J. M.; Wright, P. V. *Polymer* **1973**, *14*, 589.
- Wright, P. V. *Br. Polym. J.* **1975**, *7*, 319.
- Wright, P. V. *J. Polym. Sci., Polym. Phys. Ed.* **1976**, *14*, 955.
- Blonsky, P. M.; Shriver, D. F.; Austin, P. E.; Allcock, H. R. *J. Am. Chem. Soc.* **1984**, *106*, 6854.
- Blonsky, P. M.; Shriver, D. F.; Austin, P. E.; Allcock, H. R. *Solid State Ionics* **1986**, *18/19*, 258.
- Allcock, H. R.; O'Connor, S. J. M.; Olmeijer, D. L.; Napierala, M. E.; Cameron, C. G. *Macromolecules* **1996**, *29*, 7544.
- Allcock, H. R.; Napierala, M. E.; Cameron, C. G.; O'Connor, S. J. M. *Macromolecules* **1996**, *29*, 1951.
- Allcock, H. R.; Kuharcik, S. E.; Reed, C. S.; Napierala, M. E. *Macromolecules* **1996**, *29*, 3384.
- Allcock, H. R.; Olmeijer, D. L.; O'Connor, S. J. M. *Macromolecules* **1998**, *31*, 753.
- Allcock, H. R.; Napierala, M. E.; Olmeijer, D. L.; Cameron, C. G.; Kuharcik, S. E.; Reed, C. S.; O'Connor, S. J. M. *Electrochim. Acta (Fifth International Symposium on Polymer Electrolytes)*; Thomas, J., Ed.; **1998**, *43* (10–11), 1145.
- Allcock, H. R.; O'Connor, S. J. M.; Napierala, M. E.; Cameron, C. G.; Olmeijer, D. L. U.S. Patent 5,567,783.
- Abraham, K. M.; Alamgir, M.; Perrotti, S. J. *J. Electrochem. Soc.* **1988**, *135*, 535.
- Abraham, K. M.; Alamgir, M. *Chem. Mater.* **1991**, *3*, 339.
- Gao, L.; Macdonald, D. D. *J. Electrochem. Soc.* **1997**, *144*, 1174.
- Watanabe, M.; Kanba, M.; Nagaoka, K.; Shinohara, I. *J. Polym. Sci., Polym. Phys. Ed.* **1983**, *21*, 939.
- Abraham, K. M.; Alamgir, M. *J. Electrochem. Soc.* **1990**, *5*, 1657.
- Munshi, M. Z. A.; Owens, B. B. *Solid State Ionics* **1988**, *26*, 41.
- Xue, R.; Huang, H.; Huang, X.; Chen, L. **1994**, *74*, 133.
- Wu, P.; Holm, S. R.; Duong, A. T.; Dunn, B.; Kaner, R. B. *Chem. Mater.* **1997**, *9*, 1004.
- Allcock, H. R.; Ravikiran, R.; O'Connor, S. J. M. *Macromolecules* **1997**, *30*, 3184.
- Handbook of Chemistry and Physics*, 66th ed.; Weast, R. C., Ed.; CRC Press: Boca Raton, FL, 1985.
- Florjanczyk, Z.; Zygałło-Monikowska, E.; Raducha, D.; Such, K.; Wiczeorek, W. *Electrochim. Acta* **1992**, *9*, 1555.
- Abraham, K. M.; Alamgir, M. *Solid State Ionics* **1994**, *70/71*, 20.
- Choe, H. S.; Giaccari, J.; Alamgir, M.; Abraham, K. M. *Electrochim. Acta* **1995**, *40*, 2289.
- Abraham, K. M.; Alamgir, M.; Choe, H. S. U.S. Patent 5,474,860.
- Allcock, H. R.; Evans, T. L.; Fuller, T. J. *Inorg. Chem.* **1980**, *19*, 1026.
- Allcock, H. R.; Fuller, T. J.; Evans, T. L. *Macromolecules* **1980**, *13*, 1325.
- Montoneri, E.; Gleria, M.; Ricca, G.; Pappalardo, G. C. *J. Macromol. Sci. Chem.* **1989**, *A26* (4), 645.
- Allcock, H. R.; Fitzpatrick, R. J. *Chem. Mater.* **1991**, *3*, 1120.
- Allcock, H. R.; Klingenberg, E. H.; Welker, M. F. *Macromolecules* **1993**, *26*, 5512.
- Allcock, H. R.; Chang, J. Y. *Macromolecules* **1991**, *24*, 993.
- Allcock, H. R.; MacIntosh, M. B.; Klingenberg, E. H.; Napierala, M. E. *Macromolecules*, submitted.
- Allcock, H. R.; Scopelianos, A. G. *Macromolecules* **1983**, *16*, 715.
- Olshavsky, M. A.; Allcock, H. R. *Chem. Mater.* **1997**, *9*, 1367.
- Allcock, H. R.; Austin, P. E.; Neenan, T. X.; Sisko, J. T.; Blonsky, P. M.; Shriver, D. F. *Macromolecules* **1986**, *19*, 1508.
- Allcock, H. R.; Napierala, M. E.; Olmeijer, D. L.; Best, S. A.; Merz, K. M. *Macromolecules*, submitted.
- Allcock, H. R.; Cannon, A. M.; Olmeijer, D. L.; Diefenbach, U. In progress.
- Allcock, H. R.; Austin, P. M. *Macromolecules* **1981**, *14*, 1616.
- Hergenrother, W. I.; Halasa, A. F. U.S. Patent 4,182,837.
- Greenbalgh, R. P. *Synlett* **1992**, *7*, 235.
- Urunker, E. J.; Brehm, I.; Niu, Q. J.; Fréchet, J. M. J. *Macromolecules* **1997**, *30*, 1304.
- Allcock, H. R.; Krause, W. E. *Macromolecules* **1997**, *30*, 5683.
- Huang, B.; Wang, S.; Huang, X.; Xue, R.; Chen, L. *J. Electrochem. Soc.* **1997**, *144*, 44.
- Huang, B.; Wang, Z.; Chen, L.; Xue, R.; Wang, F. *Solid State Ionics* **1996**, *91*, 279.
- Ratner, M. A.; Shriver, D. F. *Chem. Rev.* **1988**, *88*, 109.
- Gray, F. M. *Solid Polymer Electrolytes*; VCH Publishers: New York, 1991.
- Vogel, H. *Phys. Z.* **1921**, *22*, 645.
- Tammann, V. G.; Hesse, W. Z. *Anorg. Allg. Chem.* **1926**, *156*, 245.
- Fulcher, G. S. *J. Am. Ceram. Soc.* **1929**, *8*, 339.
- Bruce, P. G.; Vincent, C. A. *J. Chem. Soc., Faraday Trans.* **1993**, *89*, 3187.

- (53) Watanabe, M.; Ogata, N. In *Polymer Electrolyte Reviews—1*; MacCallum, J. R., Vincent, C. A., Eds.; Elsevier Applied Science: London, 1987.
- (54) Watanabe, M.; Ikeda, J.; Shinohara, I. *Polym. J.* **1983**, *15*, 65.
- (55) Watanabe, M.; Ikeda, J.; Shinohara, I. *Polym. J.* **1983**, *15*, 175.
- (56) Watanabe, M.; Sanui, K.; Ogata, N.; Kabayashi, T.; Ohtaki, Z. *J. Appl. Phys.* **1985**, *57*, 123.
- (57) Watanabe, M.; Sanui, K.; Ogata, N. *Macromolecules* **1986**, *19*, 815.
- (58) Watanabe, M.; Oohasi, S.; Sanui, K.; Ogata, N.; Kobayashi, T.; Ohataki, Z. *Macromolecules* **1985**, *18*, 1945.
- (59) Allcock, H. R.; Kugel, R. L. *J. Am. Chem. Soc.* **1965**, *87*, 4216.
- (60) Allcock, H. R.; Austin, P. E.; Neenan, T. X.; Sisko, J. T.; Blonsky, P. M.; Shriver, D. F. *Macromolecules* **1986**, *19*, 1508.
- (61) McBee, E. T.; Okuhara, K.; Morton, C. J. *Inorg. Chem.* **1966**, *5*, 450.

MA980758R